

## Supporting Information for:

### Van Hove Singularities and Excitonic Effects in the Optical Conductivity of Twisted Bilayer Graphene

Robin W. Havener<sup>†</sup>, Yufeng Liang<sup>‡</sup>, Lola Brown<sup>§</sup>, Li Yang<sup>‡</sup>, Jiwoong Park<sup>\*,§,¶</sup>

<sup>†</sup>*School of Applied and Engineering Physics, Cornell University, Ithaca, NY 14853, United States,*

<sup>‡</sup>*Department of Physics, Washington University in St. Louis, St. Louis, MO 63130, United States,*

<sup>§</sup>*Department of Chemistry and Chemical Biology, and <sup>¶</sup>Kavli Institute at Cornell for Nanoscale Science, Cornell University, Ithaca, NY 14853, United States*

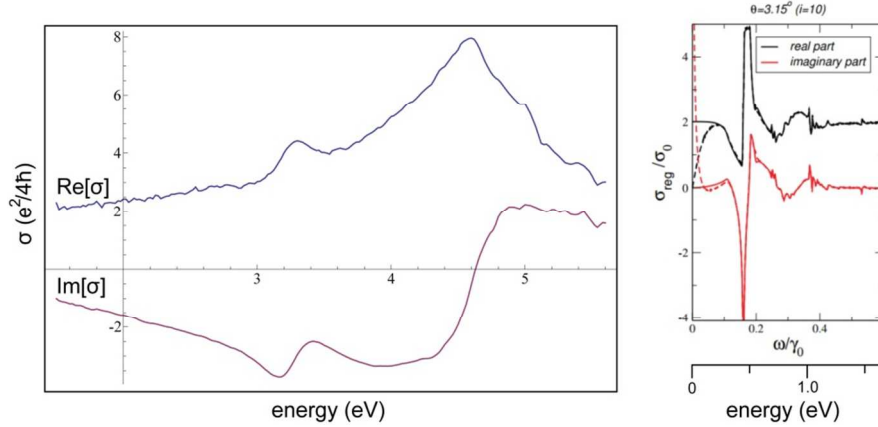
\*Correspondence should be addressed to [jpark@cornell.edu](mailto:jpark@cornell.edu)

#### (1) Methods:

Optical spectroscopy of tBLG domains was performed using the DUV-Vis-NIR hyperspectral microscope described in Ref. [1]. In summary, monochromated light from a UV-enhanced xenon arc lamp (KiloArc, OBB Corp.) illuminates the sample, and a series of images is taken as the wavelength of the light is scanned across the selected range. A long pass filter is used at wavelengths above 680 nm to eliminate the second order diffraction from the monochromator. Reflective optics, including reflective objectives, are used to eliminate chromatic aberrations. The spatial resolution of our microscope is roughly  $\lambda$ , and the optical response is averaged spatially over tBLG domains which are typically a few microns or larger in size. A series of background images is taken on a bare sample, and used to normalize the data in order to remove both spatial and wavelength-dependent variations in light intensity.

In order to facilitate TEM characterization, our graphene samples are transferred to 10 nm thick silicon nitride membranes, as discussed in the main text. Optically, these membrane substrates have the unique property that the contrast (defined as  $(I_g - I_s)/I_s$ , where  $I_g$  is the intensity of light reflected or transmitted from the graphene + substrate and  $I_s$  is the light intensity from the substrate alone) of graphene in a transmitted light image is approximately proportional to  $\text{Re}[\sigma]$ , while the contrast of graphene in a reflection image is approximately proportional to  $\text{Im}[\sigma]$ . In order to determine the full optical conductivity, we obtain both transmission and reflection spectra of the same sample. Then, we model both the reflection and transmission of the thin film sample using transfer matrices [2], leaving  $\text{Re}[\sigma]$  and  $\text{Im}[\sigma]$  of the graphene as unknowns. With these two equations, we solve simultaneously for the  $\text{Re}[\sigma]$  and  $\text{Im}[\sigma]$  at each wavelength that best fit both the reflection and transmission spectra. As discussed in the Supplementary Information of Ref. [1], we must include an additional layer in our model to account for organic residue trapped on and/or under the graphene surface. The typical thickness of this layer is 1-2 nm. The inclusion of this extra layer adds a roughly constant offset to  $\text{Im}[\sigma]$ , but has little effect on  $\text{Re}[\sigma]$ , the focus of this manuscript.

## (2) Full optical conductivity:



As outlined above, we perform both reflection and transmission spectroscopy on our samples sitting on 10 nm thick silicon nitride membranes, which we then use to obtain both the real and imaginary part of the optical conductivity ( $\sigma$ ). The figure above shows both  $\text{Re}[\sigma]$  and  $\text{Im}[\sigma]$  for one 20.5° tBLG domain on resonance. For comparison, we have reproduced theoretical predictions of  $\text{Re}[\sigma]$  and  $\text{Im}[\sigma]$  for 3.15° tBLG from Stauber *et al.* [3]. Here,  $\sigma_0$  is the universal monolayer conductivity ( $e^2/4h$ ) and  $\gamma_0 = 2.78$  eV.

The overall shapes of our experimental data and the predicted results match, although there are finer features in the calculated spectra that we do not observe due to experimental broadening as well as the difference in  $\theta$ . Because  $\text{Im}[\sigma]$  can also be calculated from  $\text{Re}[\sigma]$  through Kramers-Kronig relations over our large spectral range, we do not discuss  $\text{Im}[\sigma]$  further in the main text.

## (3) Details of continuum model fit to peak energies:

We model the band structure of SLG using the third-nearest-neighbor tight binding parameters from [4], which were fit to a first-principles GW calculation of the few-layer graphene band structure. Then, we calculate  $E_A$  and  $E_B$  as the local minima in the difference between the conduction and valence band energies,  $E_c - E_v$ , along  $I_A$  and  $I_B$ , respectively. The 4% increase in energy required for the best fit to our data is most likely necessary because the parameters in Ref [4] were fit to the calculated band structure of graphite, while weaker screening in SLG and BLG slightly increases the band energies. Our renormalized TB model provides a Fermi velocity ( $v_F$ ) of  $1.03 \times 10^6$  m/sec, similar to previous results for SLG [5,6].

## (4) Simulation details of the first-principles calculations:

Because of the demanding computational requirements of many-body calculations, our first-principles simulations consider two twisted bilayer graphene (tBLG) structures with the smallest commensurate unit cells, whose rotational angles are 21.8° and 27.8°, respectively. As the starting point, we use density functional theory (DFT) within the local density approximation (LDA) [7] to perform a structural relaxation, and obtain ground-state eigenvalues and wave functions. The DFT/LDA plane-wave cutoff is set to be 60 Ry. The atomic structures of tBLG are fully relaxed until the force on each atom is below 0.01 eV / Å. Since the degree of coupling between layers depends sensitively on the interlayer distance, we have also employed a van der Waals (vdW) functional [8], which should more accurately describe the interlayer interactions in graphene, to check whether the calculated interlayer distance is affected. Our simulation shows that the vdW-calculated interlayer distance (0.335 nm) is similar to that from

DFT/LDA, and that it is not sensitive to the twist angle ( $0.335 \pm 0.002$  nm for  $21.8^\circ$  vs.  $0.336 \pm 0.002$  nm for  $27.8^\circ$ ). However, since the conventional GW-BSE framework is incompatible with the nonlocal vdW functional, we use DFT/LDA throughout the main text for consistency.

The single-shot GW-Bethe-Salpeter equation (BSE) approach is applied to obtain the quasiparticle band structures and optical absorption spectra. The static screening is included by the Alder-Wise form of the polarizability within the random-phase approximation (RPA). It is extended to the dynamical screening calculation for the quasiparticle-energy based on the general plasmon pole model (GPP) [9]. For these plane-wave simulations, the dielectric function is expanded with a 6-Ry energy cutoff. The  $30 \times 30 \times 1$  and  $18 \times 18 \times 1$  k-point grids are employed to calculate the dielectric functions and electron-hole (e-h) interaction kernels of  $21.8^\circ$  and  $27.8^\circ$  tBLGs, respectively. Additionally, the finer k-point grids are necessary to obtain the smooth optical absorption spectra of tBLG ( $60 \times 60 \times 1$  for  $21.8^\circ$  and  $36 \times 36 \times 1$  for  $27.8^\circ$ ). Finally, e-h interactions and optical absorption spectra are obtained by solving the BSE within the Tamn-Dancoff approximation [10]. Slab Coulomb truncation is applied to avoid artificial interactions between quasiparticles of adjacent unit cells [11].

To reproduce the optical spectra across the full range of the relevant energy windows (0-6eV), we must include enough conduction and valence bands (7 bands each for  $21.8^\circ$  and 12 each for  $27.8^\circ$ ). Meanwhile, for optical absorption spectra, we only consider the case of incident light with a polarization parallel to the graphene plane because of the depolarization effect [12].

#### References:

- [1] R. W. Havener, C. J. Kim, L. Brown, J. W. Kevek, J. D. Sleppy, P. L. McEuen, and J. Park, *Nano Lett.* **13**, 3942 (2013).
- [2] Born, M.; Wolf, E., *Principles of optics: electromagnetic theory of propagation, interference and diffraction of light.* Oxford, Pergamon Press, 1964.
- [3] T. Stauber, P. San-Jose, and L. Brey. *New J. Phys.* **15**, 113050 (2013)
- [4] A. Gruneis, C. Attaccalite, L. Wirtz, H. Shiozawa, R. Saito, T. Pichler, and A. Rubio, *Phys. Rev. B* **78**, 205425 (2008).
- [5] D. Miller, K. Kubista, G. Rutter, M. Ruan, W. de Heer, P. First, and J. Stroscio, *Science* **324**, 924 (2009)
- [6] A. Luican, G. Li, A. Reina, J. Kong, R. Nair, K. Novoselov, A. Geim, and E. Andrei, *Phys. Rev. Lett.* **106**, 126802 (2011)
- [7] W. Kohn and L. Sham, *Phys. Rev.* **140**, A1133 (1965).
- [8] V. Cooper, *Phys. Rev. B* **81**, 161104(R) (2010).
- [9] M. Hybertsen and S. Louie, *Phys. Rev. B* **34**, 5390 (1986).
- [10] M. Rohlfing and S. Louie, *Phys. Rev. B* **62**, 4927 (2000).
- [11] S. Ismail-Beigi, *Phys. Rev. B* **73**, 233103 (2006).
- [12] L. Yang, C. D. Spataru, S. G. Louie, and M. Y. Chou, *Phys. Rev. B* **75**, 201304 (2007).